Dynamic measurements of the platelet membrane glycoprotein II_b-III_a receptor for fibrinogen by flow cytometry

II. Platelet size-dependent subpopulations

Mony Frojmovic and Truman Wong
Department of Physiology, McGill University, Montreal, Quebec, Canada H3G 1Y6

ABSTRACT Platelet aggregation has previously been shown to occur within 1 s of activation with 100 μM adenosine diphosphate (ADP) for both large (L) and small (S) platelet subpopulations, but L platelets were about twofold more sensitive and more rapidly recruited into microaggregates than were S platelets after correcting for differences in platelet surface area. Because platelet aggregation normally requires fibrinogen binding to glycoprotein II_b-III_a receptors (FbR) expressed on the activated platelet surface, we wished to compare the kinetics and nature of FbR expression induced by ADP for L versus S platelets, and to measure size-dependent differences in FbR expression for platelets maximally activated with phorbol myristate acetate (PMA). We presented the theory and methodology in Part I (Frojmovic, M., T. Wong, and T. van de Ven. 1991. *Biophys. J.* 59:815–827) for measuring the rate of FbR expression (k_1) and both the rate (k_2) and efficiency (α) of binding of PAC1 to FbR as a function of activation conditions from the initial on-rate of FITC-PAC1 to FbR (V) and the maximal number of FbR expressed: these are measured, respectively, from the initial rate of increase in platelet-bound fluorescence (v) and the maximal increase in mean fluorescence (Fl_{max}). We extended these analyses to L and S platelets, selected by electronic gating of forward scatter profiles (FSC), with corresponding fluorescence (Fl) histograms retrieved analytically. Platelet size (V) and surface area (SA), determined directly for cells separated with a cell sorter, were highly correlated with FSC, allowing v and Fl_{max} values to be expressed per unit area of membrane for L:S comparisons. Surprisingly, ADP activation appeared to express all FbR within 1–3 s of ADP activation for both L and S platelets, whereas k_1 was similar for PMA activation. In addition, L platelets maximally expressed two and three times more FbR per unit area than did S platelets when maximally stimulated, respectively, with ADP or PMA. Whereas k_2 was independent of platelet size for a given activator, the efficiency of PAC1 binding (α), per unit area of membrane, was two times greater for L than for S platelets, for either ADP or PMA activation. Our data suggest that the FbR structure, its microenvironment, or its surface organization may vary with platelet size or activator type. Major reorganization of FbR and/or its environment appears to occur after ~5 min of ADP activation equally for both L and S platelets. A model is presented to account for size-dependent differences in FbR expression with implications for regulation of platelet aggregation.

INTRODUCTION

Human blood platelets show size-dependent heterogeneity in structure, biochemistry, and function (1–11a). Studies have generally been conducted by physical separation of whole platelet populations into fractions having differing mean volumes, with large variability in the extent of overlap in size between fractions (<20% [1–3] to >50% [4, 5]), and possible artifacts due to isolation procedures (1–3). Studies of platelets separated by counter flow centrifugation (elutriation) have shown that large platelets are most responsive to aggregating agents (1–3), contain highest concentrations of dense and α-granules (2), are enzymatically most active (2), appear most efficient in hemostatic effectiveness (6), and may be distinctly produced from megakaryocytes of low ploidy (7).

We recently evaluated size dependent differences in platelet aggregation by comparing platelet suspensions of different sized platelets obtained by elutriation, at similar volume fractions in order to separate intrinsic biochemical differences in platelets from simple physical geometric differences. We reported that large (L)[1] platelets were about twofold more sensitive and more rapidly recruited into microaggregates in response to

Address reprint requests to Dr. M. M. Frojmovic, Department of Physiology, McGill University, 3655 Drummond Street, Montreal, Quebec, Canada H3G 1Y6.
Presented in part at the 12th Congress of Thrombosis and Hemostasis, Tokyo, August, 1989.

[1]*Abbreviations listed in this paper:* ADP: adenosine diphosphate; AF: autofluorescence values; C: control population; F:P:fluorescein:protein, ratio in molar; Fb, FbR: fibrinogen and receptor for Fb, respectively; FITC-PAC1: fluorescein isothiocyanate-PAC1 antibody; Fl, Fl_{max}: mean fluorescence for a platelet population and maximal Fl at equilibrium binding, respectively; Fn: fibronectin; FSC: forward scatter; L: large platelets (~top 20%); M: medium platelets; PMA: phorbol myristate acetate; PRP: platelet-rich plasma; RGD: arginine-glycine-aspartate; S: small platelets (~bottom 20%); SA_p: mean geometric platelet surface area; SCCS: surface-connecting membrane; SSC: side scatter; TA: dynamics of macroaggregation; V_E, V_p: mean platelet volume determined electronically and microscopically, respectively; VWF: von Willebrand factor.

0006-3495/91/04/828/10 $2.00

adenosine diphosphate (ADP) (5–100 μM) than were small (S) platelets, when suspensions were compared at identical volume fractions, i.e., at the same total surface area of platelets (1, 8). We then suggested (1), as have others (3, 9, 10), that these differences in size-dependent subpopulations are intrinsic to the cells, and we predicted that large platelets will more readily and more quickly transform $GPII_b$-III_a surface molecules into fibrinogen receptors (FbR) than will the small platelets, at about twice the sensitivity and rate. We found that the onset for platelet microaggregation induced by ADP (5–100 μM) was <0.5 s for L or S platelets, essentially as for unfractionated platelet-rich plasma (PRP), with a rapid linear increase in rate of microaggregation out to >4 s after ADP activation (1). We therefore required a method for determining the expression of FbR within seconds of platelet activation. In addition, the method would ideally not require any physical separation of the platelets from native PRP to minimize isolation artifacts which are likely responsible for some of the controversy in the relation between platelet size and function. For example, Gear et al. (4, 5) have reported that large platelets are more sensitive but slower responders to ADP in aggregation than are small platelets, but they used platelets separated functionally and by differential centrifugation.

The method that best meets the above experimental requirements is flow cytometry. We successfully used the theoretical and experimental approach, developed in Part I (11b), for measuring the dynamics of rapid expression of the FbR on platelets activated with ADP or phorbol myristate acetate (PMA) as a function of platelet size; different-sized platelets are "electronically gated" from the forward scatter properties (FSC) of the whole platelet population. We determined, by direct microscopy, the mean platelet volume and surface area of L and S platelets physically separated with a cell sorter selected by FSC. We could thus express fibrinogen receptor (FbR) expression per unit area of membrane. We then determined maximal on-rates (v_{max}) and fluorescence (Fl_{max}) for fluorescein isothiocyanate-PAC1 antibody (FITC-PAC1) binding to platelets activated with ADP or PMA for L and S platelets. This allows a comparison of rates of FbR expression (k_1), and rates (k_2) and efficiencies (α) of binding of PAC1 to FbR as a function of platelet size and activator. We found that L platelets maximally express two and three times more FbR per unit area than do S platelets in response to ADP and PMA, respectively; however, maximal expression occurs within ~1–3 s for ADP activation and at comparable rates for PMA activation, independent of platelet size. These FbR sites appear ~2–10 times more accessible to the PAC1 reporting probe depending on activator type and platelet size. A model is proposed for these differences.

METHODS

Platelet isolation and analysis by flow cytometry

The procedures used are described in Part I (11b), with the data derived from studies of six donors evaluated in Part I (11b) for both PMA (0.2 μM) and ADP (100 μM) for FITC-PAC1 preparation one, $m_o = 24$ μg/ml (F:P = 7.0).

Size-dependent subpopulations

To establish that forward scatter is a valid parameter to define size-dependent platelet fractions, cell sorting was performed on a FACS III (Becton-Dickinson Canada, Mississauga, Ontario) flow cytometer for a glutaraldehyde-fixed platelet suspension. Cell sorter gates were determined from a forward scatter histogram to obtain the lower and upper 20% forward-scattering platelets (see Figs. 1 and 2*A*). These end fractions were collected from sorting and their mean platelet volumes were determined from phase-contrast microscopy. The mean size of the upper and lower forward scattering platelets correspond to the smallest (S) and largest (L) platelets, respectively (Fig. 2*A*). Subsequent size-dependent subpopulations (each ~20% of the whole population) were analyzed by similar gating of forward scatter histograms of whole populations after data acquisition with the FACSTAR or FACSCAN, analytic instrument (Becton-Dickinson Canada).

Size analysis of platelets

The fixed platelets sorted above were analyzed by phase-contrast microscopy, using video recording and computer analyses, as previously described to measure individual platelet thickness (t), diameter (d), from which were calculated the mean axial ratio ($r_p = t/d$), geometric volume (V_p) and surface area (SA), determined for at least 100 individual platelets (unactivated disc-shaped platelets) (11).

RESULTS

Correlation of platelet forward scatter and geometric platelet size

To analyze the binding of FITC-PAC1 to platelets from the fluorescence associated with different sized platelets, we selected platelet size by obtaining FSC histograms for a given PRP preparation, and then "gating" to analytically select the 20% of platelets with the smallest (S) or largest (L) FSC intensities, as shown in Fig. 1.

Although it is known that the FSC of biological particles generally increases with the size of the particle (12, 13), this parameter cannot be used as a measure of actual platelet volume due to variable contributions from particle shape, internal structure, and refractive index (12–14). Because we also required a knowledge of platelet surface area for L and S platelets, we determined the relationship of FSC to platelet geometric size

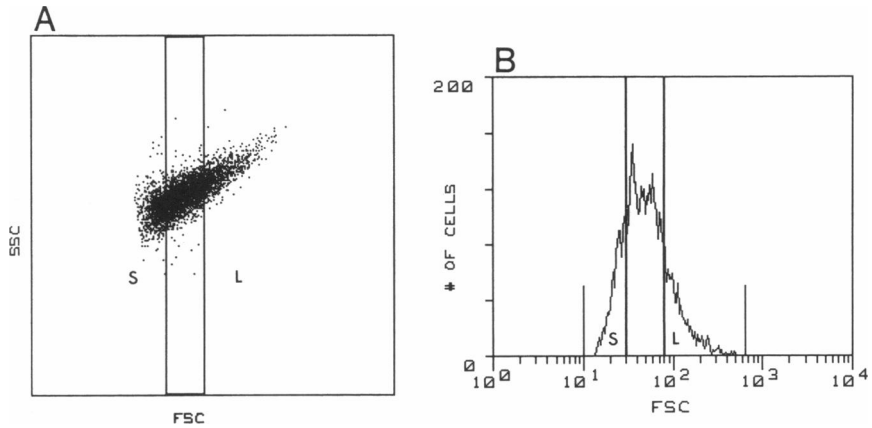

FIGURE 1 Electronic gating of different sized platelets from forward scatter intensities. Unactivated human PRP, freshly fixed with glutaraldehyde, was analyzed with a FACSTAR/sorter. In *A* the forward scatter (FSC) versus side scatter (SSC) cross-plot was obtained to identify all platelets present outside the lower threshold noise and free of other blood cells (see Methods). Platelets with the smallest and largest FSC, shown in the rectangles in *A*, were selected by setting gates on the FSC histogram shown in *B*, to represent the bottom and top 20% of forward scattering particles (S and L, respectively).

directly for platelets physically separated with the cell sorter. No platelets could be isolated by cell sorting in the absence of fixation, presumably because unfixed platelets cannot survive this isolation procedure. However, the FSC histograms were not significantly different for fixed or unfixed PRP. There was no significant change in the FSC or mean fluorescence (Fl) profiles of these fixed platelets with cell sorting (Fig. 2). The Fl was well above autofluorescence values for unfixed platelets due to Fl induced by the glutaraldehyde fixation, which was useful in providing a second parameter of platelet size, similar to that previously reported by Holme et al. (13). In fact, relative values for L and S platelets were identical for both Fl and FSC parameters (ratio of 1.23), as shown in Table 1. The geometric size was determined for these "sorted" platelets by direct microscopy (Table 1). Three fractions were actually isolated by cell sorting, and their V_p, determined for small (S), medium (M), and large (L) platelets, were shown to be highly linearly correlated with their mean FSC intensities, as well as with mean fixative-induced Fl values (Fig. 3). We thus certified that FSC, for normal platelet populations, does correlate with platelet size and we could now express Fl values per unit area of platelet for L versus S platelets.

However, we also needed to demonstrate that the largest and smallest 20% of platelets could be "selected" by "gating" FSC for platelets that had been activated with ADP or PMA. We "selected" L, M, and S platelets by "gating" for the 20% of fixed platelets with the highest and lowest values of FSC or autofluorescence (Fl), as well as for one third of all platelets yielding the midrange values for the whole population. This was done for the same donor's platelets for control or activated with ADP or PMA. If the linear relation of FSC or Fl with size shown in Fig. 3 for unactivated platelets physically separated by size was equally valid for activated platelets, then the "gating" for size by FSC should also yield a linear correlation between FSC and Fl, independent of activation, as shown in Fig. 4. Plots of FSC or Fl versus V_p of the "resting" platelets (obtained from Fig. 3) also gave linear correlations for L, M, and S platelets ($r = 0.95$), independent of activation (curves not shown). Finally, because we "select" L and S platelets by "gating" on FSC for unfixed, activated platelets, it is important to note that mean FSC values increased by $< 8 \pm 4\%$ when comparing fixed platelets with unfixed platelets, independently of activation or platelet size.

The possible complications of platelet aggregation were shown to be negligible in Part I (11b) ($< 5\%$ aggregation occurred in all cases). We reanalyzed mean Fl values for ADP or PMA activated L platelets, "selected" as particles with the top 15–20% of FSC values after "gating" out the top 5% of FSC values, and found $< 20\%$ decreases in Fl with such exclusion.

Distinct kinetics and extent of FITC-PAC1 binding for L and S platelets

The overall time course of specific FITC-PAC1 binding to activated platelets was determined for PAC1 incubation times varying from 5 s out to 30 min by dilution quenching PRP samples containing activator and PAC1 and obtaining fluorescence histograms for each of these time points (reported in Part I [11b]). We then analyzed

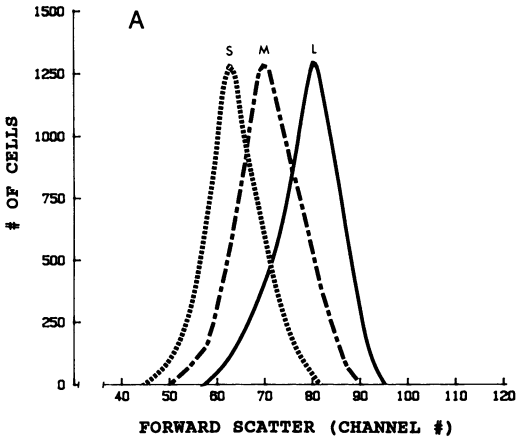

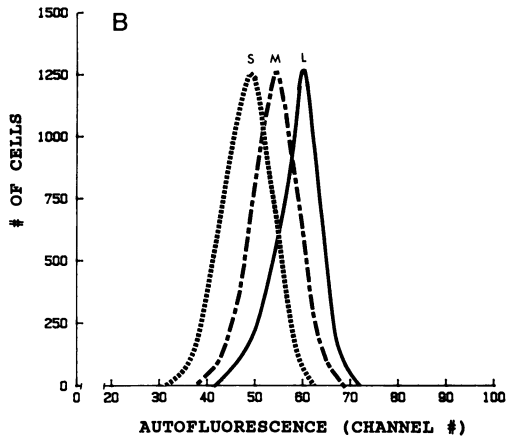

FIGURE 2 Forward scatter and autofluorescence histograms of fixed platelets before and after cell sorting. Using the electronic gating procedure shown in Fig. 1, fixed platelets in PRP were analyzed for (*A*) FSC and (*B*) autofluorescence (Fl) for the bottom 20% (S) and top 20% (L) of particles analyzing FSC and Fl intensities histograms independently, as well as the midfraction contain one-third of all platelets (M).

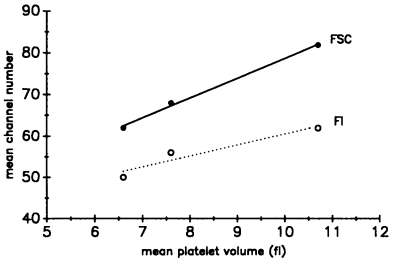

FIGURE 3 Platelet forward scatter is highly correlated with geometric platelet volume. S, M, and L sized platelets were physically fractionated with the FACS III (Becton-Dickinson Canada) cell sorter using their FSC properties described in Fig. 2 and Table 1. The mean geometric volume measured by direct microscopy for each of these three fractions was plotted against the corresponding mean FSC or mean autofluorescence, Fl (data in Table 1), giving a linear regression plot ($r = 0.95, p < 0.05$ for each of the two curves).

these fluorescence histograms by plotting the Fl histograms corresponding to the L and S platelets selected from FSC profiles (Fig. 5). Fl values were thus determined for these L and S subpopulations, shown for one donor's PRP in Fig. 5 which had been incubated with 100 μM ADP and FITC-PAC1 for 30 min. Platelets were first maximally preactivated for a time τ with PMA for 25 min or with ADP for 0–10 s. Fl time plots for such preactivated platelets are shown for typical donors for PMA (Fig. 6 *A*) and for ADP (Fig. 6 *B*), where Fl values are shown for the whole control population (C), as well as for the L and S platelets. The initial increase in Fl measured for $t < 15$ s of PAC incubation yields the maximal initial on-rates for PAC1 binding (v_{max}), as described in Part I (11 b). It is seen that both S and L platelets gave significant Fl values within 5 s of ADP activation, with distinct values for v_{max} and for the maximal increase in Fl by 30 min of PAC1 incubation, Fl_{max}. These values for initial on-rates (v_{max}) and maximal

TABLE 1 Relation of platelet forward scatter (FSC) to platelet geometric size

Platelet subpopulation	Flow cytometry* Fl‡ Pre	Fl‡ Post	FSC§ Pre	FSC§ Post	Microscopy geometry of sorted cells‖ Volume	Shape¶	Surface area
	FU		*CN*		*fl*		μm^2
Top 20% (L)	61	62	77	79	10.8	0.38	26.2
Bottom 20% (S)	50	50	64	62	6.6	0.35	19.4
L:S	1.22	1.24	1.20	1.27	1.64	1.09	1.35

*Flow cytometry values for Fl and FSC are reported for the fixed platelets analyzed pre- and postcell sorting, with histograms shown in Fig. 2 (FACS III [Becton-Dickinson Canada] cell sorter). The middle 33% of the population (M) had Fl, FSC, and V values of 56, 71, and 7.7 μm^3 respectively (pre or post); ‡Fl = mean Fl due to autofluorescence of GA fixed platelets, expressed in fluorescence units (FU); §log normal distribution of FSC histograms where mean channel number (CN) is reported; ‖the fixed cells were sorted according to their FSC profiles into a L and S population and measured directly by microscopy (see Methods); ¶the shape refers to the axial ratio, expressed as average r_p, the ratio of platelet thickness (t) to diameter (d).

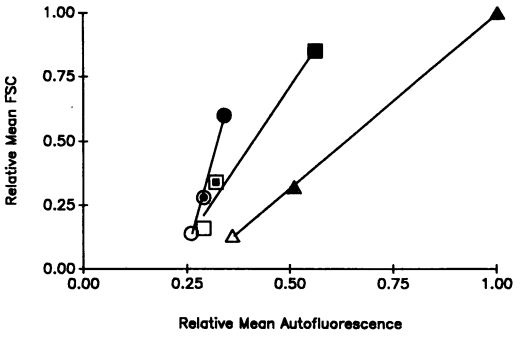

FIGURE 4 Platelet size "selected" by FSC correlates linearly with autofluorescence for control, ADP or PMA-activated platelets. Platelets were fixed for PRP control (*circles*), and for PRP maximally preactivated with ADP (*squares*; 100 μM, $\tau = 15$ min) and PMA (*triangles;* 0.2 μM, $\tau = 45'$). The large (●, ■, ▲), medium (⊙, ▣, ◬) and small (○, □, △)-sized platelets were "selected" from the top 20%, midfraction containing one-third of all platelets, and bottom 20%, respectively. The mean FSC values and corresponding autofluorescence values (AF) were determined from the "selected" populations. The FSC and AF were linearly correlated for control, ADP and PMA samples ($r = 0.99, p < 0.05$).

binding (Fl_{max}) are summarized in Table 2 for six donors, each donor's PRP evaluated for both ADP and PMA activation. It is seen that L platelets have both v_{max} and Fl_{max} values which are three and four times greater than those for small platelets, for ADP and PMA activation, respectively. Part of this difference resides in the ~1.4-fold difference in surface area of L:S platelets (Table 1); however, normalizing for this difference still yields a two and three times greater v_{max} or Fl_{max} values for L platelets

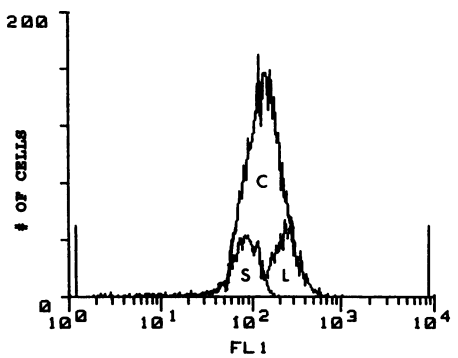

FIGURE 5 Analysis of FITC-PAC1 binding for size dependent subpopulations by flow cytometry. Platelet-rich plasma was incubated with 100 μM ADP and FITC-PAC1 (added together for 30 min to yield fluorescence) histogram (C) due to PAC1 bound to the maximally activated platelets. By electronically gating for the top (L) and bottom (S) 20% of forward scattering particles (Figs. 1 and 2), the corresponding fluorescence histograms can then be obtained for these S and L platelets, as shown.

than for S platelets, respectively, for ADP and PMA activation.

As shown in Part I (11b), the ratios of v_{max} to Fl_{max} values actually represent k_2 values for on-rates of PAC1 to maximally preactivated platelets which are summarized as relative values for L versus S platelets in Table 3 (k_2^L/k_2^S). Thus, k_2 appears approximately independent of platelet size for both ADP and PMA activation, as is the case of analyses of the rate of expression of FbR sites for PMA (k_1 values [Table 3]). For ADP activation, k_1 was $> 20\ \text{min}^{-1}$ for both L and S platelets but actual ratios could not be determined as maximal FbR expression appears to occur in < 3 s for both L and S platelets. However, the maximal numbers of PAC1-binding sites (Fl_{max}) expressed per unit area of membrane are approximately two and three times greater for ADP and PMA activation, respectively.

We also obtained the relative efficiencies of L versus S platelets (α^L/α^S) from the relative on-rates (v_{max} values in Table 2) but corrected for differences in platelet size: we found that maximally activated L platelets bound PAC1 about two times more efficiently than did S platelets, for either ADP or PMA activation (Table 3).

We finally compared Fl_{max}, k_2, and α values for ADP versus PMA activation for the whole platelet population as well as for L and S platelets, obtained for the same platelet preparation from each of six donors (Table 4). We found that whereas PMA causes approximately twofold more PAC1 maximal expression for L platelets than does ADP, there is only about a 1.4-fold increase in Fl_{max} for the S platelets; the whole population shows intermediate differences for PMA versus ADP (see Fl_{max} ratios in Table 4). Although the rate constant for PAC1 binding to platelets maximally activated with PMA (k_2) was two to three times greater than for activation with ADP for the large or total platelet population, it appeared to be approximately four times greater for activation of small platelets (relative k_2 values in Table 4). This size-dependent difference was not apparent in relative efficiencies, where PMA activation causes approximately fivefold greater increases in α than does ADP activation, for L or S platelets.

Time dependent decay in v_τ after activation with ADP

We reported in Part I (11b) that initial rates of increase in Fl, (v_τ), appeared to be maximal within ~1–3 s of ADP activation of platelets, but that v_τ values then decayed by >50% if platelets were preactivated for 15 min before addition of PAC1, with no significant change, however, in Fl_{max} values. These changes were ascribed to changes in accessibility of the $GPII_b$-III_a FbR to FITC-PAC1 due to further conformational, microenvironmen-

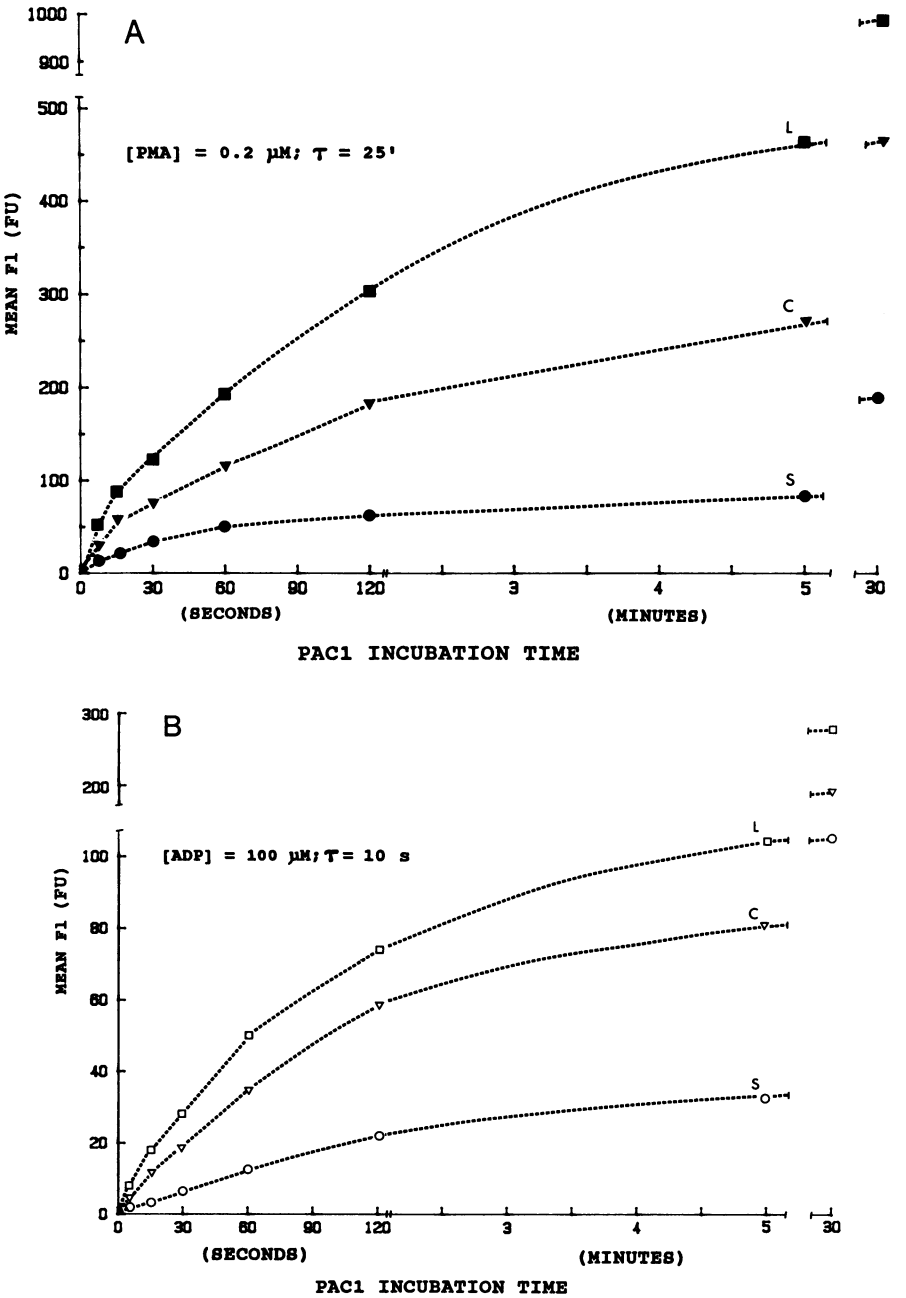

FIGURE 6 Dynamics of fibrinogen receptor expression on L versus S platelets for activation with (*A*) ADP and (*B*) PMA. Human PRP was preactivated at times (τ) yielding maximal initial rates of PAC1-binding and maximal expression of PAC1-binding sites (Table 2); this corresponded to τ = 1–10 s and 25 min for ADP and PMA, respectively. Activated PRP were then incubated for varying times τ with FITC-PAC1, dilution quenched and analyzed in the flow cytometer. The mean fluorescence (Fl) was then determined from fluorescence histograms for each time point for the whole population (control C), as well as for the L and S platelets selected as the top and bottom 20% from FSC profiles (see Fig. 4). These plots of Fl versus PAC incubation time are shown for one representative donor for each activator.

tal or clustering effects, which could reduce v values (on-rates) while not actually showing refractoriness or disappearance of maximal numbers of FbR expressed (Fl_{max}). We found a similar "decay" (~30–40%) occurring in initial on-rates (v) of PAC1 binding to activated platelets after 5–15 min of activation with ADP for the whole (total) population and for L or S platelets (Table 5). Moreover, Fl_{max} was unchanged with time after ADP

TABLE 2 **Size-dependent differences in PAC1 binding kinetics for maximal activation with PMA and ADP***

Platelet subpopulation‡	PMA (0.2 μM; τ = 25 min)		ADP (100 μM; τ = 0–10 s)	
	v_{max}	Fl_{max}	v_{max}	Fl_{max}
	FU/s	*FU*	*FU/s*	FU
L	6.6 ± 2.1	804 ± 231	1.5 ± 0.7	378 ± 94
S	2.0 ± 0.7	196 ± 31	0.5 ± 0.2	141 ± 13
L:S§	3.5 ± 0.6	4.1 ± 0.9	3.2 ± 0.6	2.7 ± 0.6
$L:S_{corr}$‖	2.5 ± 0.5	2.9 ± 0.6	2.3 ± 0.4	1.9 ± 0.4

*The mean ± SD is reported for pooled data for v_{max} and Fl_{max} obtained in parallel for PMA and ADP activation for each of six donors; τ = activation time of PRP before FITC-PAC1 addition; ‡L and S represent large and small platelets selected from top and bottom 20% of FSC values, as in Table 1; §L:S ratios of v_{max} and Fl_{max} values were determined for each donor and then averaged; ‖corrected by dividing by 1.4, the ratio of mean surface area for L:S (see Table 1 and Results).

activation for L or S platelets. This "decay" in v_τ reflects a comparable decrease in $k_2(\tau)$ and efficiency (α) (see Eqs. 11–14 in Part I [11b]).

DISCUSSION

We have compared the rate and extent of binding of FITC-PAC1 to its $GPII_b$-III_a FbR on platelets activated in PRP with ADP or PMA for large and small platelet subpopulations. These have been "electronically" selected from the FSC profiles of the unfixed platelets. We demonstrated that FSC correlates well with geometric platelet size (V_p) (Fig. 3) using fixed, unactivated, disc-shaped platelets whose size and shape did not change with the sorting procedure used for direct

TABLE 3 **Relative dynamics for the expression and occupancy of PAC1 binding sites for large versus small platelets**

	k_1^L/k_1^S	k_2^L/k_2^S‡	Fl_{max}^L/Fl_{max}^S§	α^L/α^S‖
ADP	—	1.3 ± 0.3	1.9 ± 0.4	2.1 ± 0.3
PMA	1.06*	0.9 ± 0.2	2.9 ± 0.6	2.1 ± 0.5

*k_1 was analyzed for one donor from Fig. 9 in Part I (11b) for the second rapid phase seen with PMA activation with 0.2 μM; k_1^L/k_1^S for the initial slow phase (see Fig. 9 in Part I [11b]) = 0.8, but k_1^L/k_1 for the whole population = 1.0, with uncertainty in k_1^S due to very low fluorescence values at early activation times; ‡k_2 values were obtained from the six donors in Table 2; $k_2 m_o$ values for L platelets were respectively 0.24 ± 0.07 and 0.60 ± 0.18 min^{-1} for ADP and PMA activation; §corrected for surface area differences (from Table 2); ‖relative efficiencies equal column 2 × column 3 divided by a_{pl}^L/a_{pl}^S = 1.18 for $V^{1/3}$ taken from Fig. 3 for resting platelets using Eqs. 12 and 13 from Part I (11b); α^L for PMA and ADP is typically ~20 and 4%, respectively.

TABLE 4 **Comparison of Fl_{max}, k_2, and α for PAC1 sites induced by PMA versus ADP for total platelets, for large and for small platelets**

Platelet size‡	Ratios of values for PMA:ADP for*		
	Fl_{max}(PMA)/ Fl_{max}(ADP)	k_2(PMA)/ k_2(ADP)	α(PMA)/ α(ADP)
Total cells	1.8 ± 0.6	1.7 ± 0.3	3.0 ± 0.6
L	2.2 ± 0.7	2.7 ± 1.7	5.3 ± 2.9
S	1.4 ± 0.2	3.9 ± 2.8	5.2 ± 3.2
L:S§	1.6‖	0.72‖	1.1 (NS)¶

*Six donors with PMA and ADP activation studied in parallel. Ratios for Fl_{max} (PMA)/Fl_{max} (ADP), as well as for k_2 and α values, were determined for each donor, and mean ± SD reported; ‡data are reported for the total population from Table 2 in Part I (11b) for the same six donors; §values of L to S platelets (L:S) were obtained for each donor and the mean ratio determined for all six donors; significance of differences were evaluated with a one-tailed paired t-test: ‖$p < 0.05$; ¶$p > 0.10$. A similar comparison of total cells: L platelets showed $p < 0.05$, > 0.1, and < 0.1, respectively, for Fl_{max}, k_2, and α ratios.

microscopic determinations of size (Fig. 2 and Table 1). This direct linear correlation of FSC and V_p is consistent with another report which demonstrated a highly significant linear correlation between FSC and mean electronic size V_E obtained for parallel samples of unfixed whole PRP for different normal human donors (13). We additionally demonstrated that FSC and fixative-induced autofluorescence both correlated linearly with size for physically sorted unactivated fixed platelets (Fig. 3), as well as for platelets maximally activated with ADP or PMA which were "selected" for size from FSC "gating" (Fig. 4). We could now compare the mean fluorescence, Fl, for L and S platelets by simple computer-driven selection of Fl values corresponding to selected FSC values (Fig. 5). This permitted a comparison of rates (v) and extent (Fl_{max}) of FITC-PAC1 binding to activated platelets as a function of platelet size for both PMA (Fig. 6 *A*) and ADP (Fig. 6 *B*). As large platelets showed three to fourfold greater values for either v_{max} or Fl_{max} compared to small platelets when maximally preactivated with either ADP or PMA (Table 2), we wished to dissociate these differences from simple physical differences due to surface area.

We found for the one donor's platelets isolated by cell sorting that the large platelets (as selected from 20% of platelets with the largest FSC) had a geometric surface area, SA_p, which was 1.35× that of S platelets. To normalize Fl values for L and S platelets for different donors, we chose an SA_p ratio of 1.4 for L:S (Table 2). This was determined as follows. We have previously demonstrated that mean electronic volumes (V_E) for L and S platelets separated by elutriation as top and

TABLE 5 **Time-dependent decay in v_τ for ADP-induced activation**

Preincubation time (θ)*	v_τ‡			Fl_{max}‡		
	Total	L	S	Total	L	S
		FU/s			*FU*	
1–3 s	1.0	1.0	1.0	1.0	1.0	1.0
5–15 min	0.69 ± 0.24§	0.71 ± 0.22	0.61 ± 0.28	1.0 ± 0.05	0.99 ± 0.02	0.95 ± 0.07

*Platelets were activated in PRP (1:10) with 100 μM ADP for different times τ preceding addition of FITC-PAC1, for three donors; ‡initial rates of Fl increase were measured for different τ values (v_τ), as well as Fl_{max} values measured for PAC1 incubation for > 30 min (see Fig. 5 and Part I [11b]); §values in this row were expressed as a fraction of the values obtained for τ = 1–35.

bottom 16–20% of the population, remained relatively constant for different donors (n = 11) (1): in fact V_E(L):V_E(S) = 1.7 ± 0.2 (n = 11). The relative surface area values for equivalent spheres becomes $V_E^{2/3}$(L):$V_E^{2/3}$(S) = 1.4 ± 0.1. It is known that V_p(L):V_p(S) = V_E(L):V_E(S) for platelets having the same shape (15) and it therefore follows that [V_p(L):V_p(S)]$^{2/3}$ = 1.4 ± 0.1 (n = 11)]. Finally, it can be calculated from Table 2 that [V_p(L):V_p(S)]$^{2/3}$ = 1.39, comparable to the value obtained from direct measures of SA_p(L):SA_p(S) = 1.35. Relative surface areas can thus be determined simply from electronically-derived V_E values. In the case of normal donors, a mean value of 1.4 ± 0.1 can confidently be used for L:S values of SA_p, especially in our studies where the five donors evaluated were chosen from this same pool of donors used for our previous report (1).

The above comparison of relative surface areas for unactivated, smooth-surfaced L and S platelets will equally be valid for activated platelets if the following conditions are satisfied: the membrane roughening and surface projections occurring with platelet activation (9, 16) do not alter the amount of membrane and associated number of FbR accessible to the reporting probe (FITC-PAC1), or any such changes occur equally for L and S platelets. The FITC-PAC1 reporting molecule is an IgM expected to penetrate the surface-connecting membrane (SCCS) reported to have pore sizes of ~500–2,000 Å (9). Therefore, the reported increases in mean surface area (~25%) occurring with platelet activation, likely associated with outflow of SCCS (9, 16), are not expected to affect total Fl measured for L or S platelets; it must be noted in this regard that a constant twofold increase in external surface area occurs with hypo-osmotic externalization of all SCCS for L or S platelets (17). Although it appears unlikely, we cannot presently rule out the possibility that L platelets selectively externalize or render accessible more SCCS (or other internal membrane pools) and associated FbR than do S platelets upon ADP and PMA activation. In such a case, the surface density of FbR for L platelets would be closer to that for S platelets only if L platelets externalized all of their SCCS.

Large platelets appear to maximally express about two times more FbR per unit area of membrane than do the small platelets when activated with ADP (Table 3), but somewhat surprisingly, ADP activation appears to express all FbR within 1–3 s irrespective of platelet size, i.e., equivalent v_{max} was observed for τ = 0, 1, 2, or 3 s for L or S platelets when analyzed as described in Part I (11b) (data not shown). Thus, the actual rate of FbR expression may be 10,000 FbR/s, all expressed within 1 s for both L and S platelets (taking 10,000 as an average number of maximal FbR expressed with ADP [18, 19]). This result is fully consistent with our previous report (1) that the onset for platelet aggregation is <0.5 s for L or S platelets but appears in conflict with the greater than twofold slower rate of aggregation of S platelets measured between 2–10 s after ADP addition (Fig. 1 in reference 1). It therefore appears that the FbR density or number per unit area may regulate the rate of platelet aggregation in the early aggregation phase (within the first few seconds of activation), rather than the rate of expression of FbR. It is additionally possible that the surface density and accessibility of FbR, which are also affected by post-Fb binding events (18), may be rate-determining in platelet aggregation, rather than the number of FbR per se, because these appear maximally expressed well before aggregation is complete. In this regard, it is important to note that the efficiency of PAC1 binding (α) to ADP-activated platelets was two times greater for L than for S platelets (Table 3), suggesting that the surface distribution and accessibility of FbR to PAC1 favor more efficient binding of PAC1 to its specific receptor on L platelets compared to S platelets once all are maximally expressed: this may reflect important structural differences in FbR and its microenvironment which favor "functional" expression of FbR-adhesive proteins. Finally, it would appear that these differences in FbR expression and organization for L versus S platelets are unrelated to the dynamics of macroaggregation (TA) insofar as TA was shown to be independent of platelet size when adjusted for surface area differences (1).

Although L platelets appear to express approximately

two to three times more PAC1 binding sites per unit area of platelet surface membrane than do S platelets after activation with ADP or PMA, the efficiencies of PAC1 binding are approximately twofold greater for L than for S platelets, for either activator (Table 3). This is not reflected in relative rate constants for PAC1 binding (k_2), which are independent of platelet surface area and appear independent of platelet size for a given activator (Table 3).

As predicted for ADP, PMA activation appears to express new FbR sites at a comparable rate for L and S platelets (relative k_1 values in Table 3). However, L platelets express approximately three times more maximal numbers of FbR sites than do S platelets (relative Fl_{max} values in Table 3). Because PMA activation causes externalization of α-granule membranes and additional $GPII_b$-III_a from the intracellular pool (18, 20), it is possible that FbR expression is also a function of platelet secretion. The report that rates of secretion are similar for L and S platelets isolated by elutriation (2) are consistent with our observation that k_1 for FbR are comparable; but we found that the final extent of FbR expression differ. Moreover, maximal FbR expression was twofold greater for L than for S platelets for ADP activation, where negligible secretion is expected (no significant platelet aggregation in our experimental conditions). In this regard, it is seen that PMA causes ~2.2 times greater maximal expression of FbR on L platelets than does ADP, with ~40% lower relative effect on S platelets (Table 4). This may reflect L platelets recruiting more FbR from internal pools (18, 20).

In addition, L platelets may be more efficient at converting the inactive $GPII_b$-III_a to its FbR form, i.e., a greater percent of all $GPII_b$-III_a are transformed for L platelets than for S platelets, as reflected in the above. However the efficiency of conversion of $GPII_b$-III_a to FbR also requires a knowledge of the surface density of all $GPII_b$-III_a molecules (inactive and FbR forms) which we are measuring with other appropriate antibodies, such as FITC-labeled AP-2 (21) and Tab (22). Our preliminary results with AP-2 and Tab suggest that surface densities of $GPII_b$-III_a on resting platelets are identical for unactivated L and S platelets, but effects of activators and of secretion of internal FbR pools must be evaluated.

The relative efficiency of PAC1 capture by PMA-activated platelets (α) is approximately five times greater than for ADP-activated platelets, whether comparing L or S platelets (compare v_{max} ratios for PMA:ADP in Table 2 and see relative α values in Table 4). Finally, either ADP or PMA-activated platelets had α values two times greater for L versus S platelets (Table 3). Thus, both platelet size and activator type can enhance the capture efficiency of FbR for PAC1 by up to 10-fold. This reflects altered FbR structure/microenvironment/surface organization favoring capture efficiency of the PAC1 molecule. It is expected that similar observations will be found with other arginine-glycine-aspartate (RGD)-containing adhesive proteins, including Fb, VWF (von Willebrand factor), and Fn (fibronectin).

The apparent decay in rates of binding of PAC1 to platelets preactivated with ADP at longer activation times ($\tau > 5$ min), compared to short activation times ($\tau \sim 1$–3 s) (Table 5), suggests that changes occur in the microenvironment or in the organization of FbR in the activated platelet surface with increasing activation time. Identical apparent changes were seen in v_τ for L and S platelets, with no decay in Fl_{max} values. This ~30–40% decay in v_τ thus corresponds to a comparable decay in both k_2 and the efficiency of PAC1 binding (α) (see Eq. 14 in Part I [11b]), suggesting that similar reorganization occurs with activation time independent of platelet size. If the poorer accessibility to these FbR by PAC1 is also reflected in fibrinogen binding, we would predict that initial rates of platelet aggregation would decrease with increasing times of preincubation with ADP. However, microaggregation has been shown to be independent of τ values (23). Moreover, these differences in v_τ and Fl_{max} appear irrelevant to L platelet aggregate build-up measured turbidimetrically (TA), as L and S platelets have been reported to yield comparable macroaggregation when corrected for effects of size (1).

The regulation of platelet aggregation and the role of the fibrinogen receptor in this regulation will be better characterized through parallel measures of platelet size, membrane rearrangements, and changes in the total number of $GPII_b$-III_a molecules and active Fb receptors as a function of pre- and post-Fb binding. This is being done with flow cytometry using appropriately selected fluorescently labeled antibodies such as S12 (24) to follow α-granule secretion.

We gratefully acknowledge the support in aid-of-research from the Medical Research Council of Canada.

We appreciate the generosity of Dr. Gerry Price (McGill Cancer Center) for the use of his FACS III Cell Sorter (Becton-Dickinson Canada, Mississauga, Ontario), and the assistance of Mr. R. McKenzie; we thank Mr. K. McDonald for technical assistance with the FACSTAR flow cytometer (Becton-Dickinson Canada). We thank Drs. S. Shattil (University of Pennsylvania), T. Kunicki (Blood Center of Wisconsin), and R. McEver (University of Oklahoma), respectively, for their generous donations of monoclonal antibodies PAC1, AP-2, and Tab.

Received for publication 12 June 1990 and in final form 10 December 1990.

REFERENCES

1. Wong, T., L. Pedvis, and M. M. Frojmovic. 1989. Platelet size affects both micro- and macro-aggregation: contributions of platelet number, volume fraction and cell surface. *Thromb. Haemostasis.* 62:733–741.
2. Thompson, C. B., K. A. Eaton, S. M. Princiotta, C. A. Rushin, and C. R. Valeri. 1982. Size-dependent platelet subpopulation relationships of platelet volume to ultrastructure, enzymatic activity and function. *Br. J. Haematol.* 50:509–519.
3. Thompson, C. B., J. A. Jakubowski, P. G. Quinn, D. Deykin, and C. R. Valeri. 1983. Platelet size as a determinant of platelet function. *J. Lab. Clin. Med.* 101:205–213.
4. Carty, D. J., and A. R. L. Gear. 1986. Fractionation of platelets according to size: functional and biochemical characteristics. *Am. J. Hematol.* 21:1–6.
5. Haver, V. M., and A. R. L. Gear. 1982. Functional fractionation of platelets: aggregation kinetics and glycoprotein labeling of differing platelet populations. *Thromb. Haemostasis.* 48:211–216.
6. Thompson, C. B. 1985. Selective consumption of large platelets during massive bleeding. *Br. Med. J.* 291:95–96.
7. Penington, D. G., K. Streatfield, and A. E. Roxburgh. 1976. Megakaryocytes and the heterogeneity of circulating platelets. *Br. J. Haematol.* 34:639–653.
8. Frojmovic, M. M. 1989. Comparative studies of turbidimetrically measured rates of platelet aggregation require adjustment of the platelet suspension according to the mean relative size and optical efficiency of the platelets used. *Blood.* 74:2302–2303.
9. Frojmovic, M. M., and J. G. Milton. 1982. Human platelet size, shape, and related functions in health and disease. *Physiol. Rev.* 2:185–261.
10. Karpatkin, S. 1978. Heterogeneity of human platelets. VI. Correlation of platelet function with platelet volume. *Blood.* 51:307–316.

11a. Frojmovic, M. M., and R. Panjwani. 1976. Geometry of normal mammalian platelets by quantitative microscopic studies. *Biophys. J.* 16:1071–1089.

11b. Frojmovic, M., T. Wong, T. van de Ven. 1991. Dynamic measurements of the platelet membrane glycoprotein II_b-III_a receptor for fibrinogen by flow cytometry. I. Methodology, theory, and results for two distinct activators. *Biophys. J.* 59:815–827.

12. Shapiro, H. H. 1985. Parameters and probes. *In* Practical Flow Cytometry. H. H. Shapiro, editor. Alan R. Liss Inc., New York. 115–199.
13. Holme, S., A. Heaton, A. Konchuba, and P. Hartman. 1988. Light scatter and total protein signal distribution of platelets by flow cytometry as parameters of size. *J. Lab. Clin. Med.* 112:223–231.
14. McGann, L. E., M L. Walterson, and L. M. Hogg. 1988. Light scattering and cell volumes in osmotically stressed and frozen-thawed cells. *Cytometry.* 9:33–38.
15. Milton, J. G., W. Yung, and M. M. Frojmovic. 1981. Dependence of platelet volume measurements in heterogeneity of platelet morphology. *Biophys. J.* 35:257–261.
16. Woods, V. L., L. E. Woolff, and D. M. Keller. 1986. Resting platelets contain a substantially centrally located pool of glycoprotein II_b-III_a complex which may be accessible to some but not other extracellular proteins. *J. Biol. Chem.* 261:15242–15251.
17. Frojmovic, M. M., T. Wong, J. Wylie, and J. G. White. 1987. Platelet external surface membrane is osmotically doubled irrespective of size or species (human/bovine): dynamics and membrane sources. *Thromb. Haemostasis.* 58:302.
18. Nurden, A. T. 1987. Platelet membrane glycoproteins and their clinical aspects. *In* Thrombosis and Haemostasis. M. Verstraete, J. Vermylen, R. Lijnen, and J. Armout, editors. Leuven University Press, Leuven, Belgium. 93–125.
19. Shattil, S. J., J. A. Hoxie, M. Cunningham, and L. F. Brass. 1985. Changes in the platelet membrane glycoprotein II_b-III_a complex during platelet activation. *J. Biol. Chem.* 260:11107–11114.
20. Wencel-Drake, J. D., E. F. Plow, T. J. Kunicki, V. L. Woods, D. M. Keller, and M. H. Ginsberg. 1986. Localization of internal pools of membrane glycoproteins involved in platelet adhesive responses. *Am. J. Pathol.* 124:324–334.
21. Pidart, D., R. R. Montgomery, J. S. Bennett, and T. J. Kunicki. 1983. Interaction of AP-2, a monoclonal antibody specific for the human platelet glycoprotein II_b-III_a complex, with intact platelets. *J. Biol. Chem.* 258:12582–12586.
22. McEver, R. P., E. M. Bennett, and M. N. Martin. 1983. Identification of two structurally and functionally distinct sites on human platelet membrane glycoprotein II_b-III_a using monoclonal antibodies. *J. Biol. Chem.* 258:5269–5275.
23. Frojmovic, M. M., J. G. Milton, and A. Duchastel. 1983. Microscopic measurements of platelet aggregation reveal a low ADP-dependent process distinct from turbidometrically measured aggregation. *J. Lab. Clin. Med.* 101:964–976.
24. Shattil, S. J., M. Cunningham, and J. A. Hoxie. 1987. Detection of activated platelets in whole blood using activation-dependent monoclonal antibodies and flow cytometry. *Blood.* 70:307–315.